



Cite this: DOI: 10.1039/c6cc03423c

Received 24th April 2016,
Accepted 3rd May 2016

DOI: 10.1039/c6cc03423c

www.rsc.org/chemcomm

Dimension-controlled assemblies of modified bipyrroles stabilized by electron-withdrawing moieties†

Kazuto Nakamura,^a Nobuhiro Yasuda^b and Hiromitsu Maeda^{*a}

Benzoyl-substituted bipyrroles possessing aliphatic chains were synthesized and formed a variety of dimension-controlled assembled structures as mesophases through various intermolecular interactions.

Assemblies comprising π -electronic molecules are essential for fabricating electronically functional materials.¹ The introduction of interacting moieties into π -electronic units can result in dimension-controlled organized structures *via* π - π stacking and other interactions. As an example, dipole-dipole interactions are important for controlling molecular orientations and resulting assembled structures.² Interaction strengths vary, resulting in unique thermal transition behaviours and related properties. We have focused on pyrrole derivatives, which possess hydrogen-bond donating NH sites, as π -electronic units that form assembled structures.³ Pyrrole rings are well-known building blocks in biotic functional dyes, such as chlorophyll and haem, in which they are stabilized by aromatic macrocycles.⁴ Therefore, the design and synthesis of stable linear oligopyrroles would be valuable for the development of π -electronic molecules and their assemblies. Although directly linked oligopyrroles are less stable due to their electron-rich states, their potential as assembly building units should be examined *via* the introduction of electron-withdrawing moieties. As an example, Geier *et al.* have reported a benzoyl-substituted pyrrole dimer (bipyrrrole) **1**, prepared from 2,2'-bipyrrrole⁵ and *N,N*-dimethylbenzamide (Fig. 1a), although properties such as assembled behaviour were not investigated in detail.⁶ Based on this background, we report the synthesis and assembled structures of bipyrroles α -substituted with modified benzoyl units (**2a-d** and **3a-d**, Fig. 1b). Aliphatic chains, such as OC₈H₁₇, OC₁₂H₂₅ and OC₁₆H₃₃, were introduced into **2b-d** and **3b-d** to

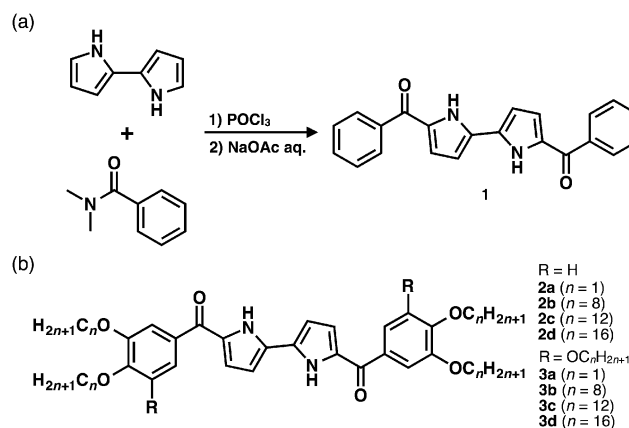


Fig. 1 (a) Synthesis and (b) structures of dibenzoylbipyrrrole derivatives.

induce van der Waals interactions, which cause the formation of dimension-controlled assemblies.

Following a literature procedure,⁶ benzoyl-substituted bipyrroles **2a-d** and **3a-d**, possessing four and six alkoxy chains, respectively, were synthesized from the corresponding benzamides⁷ in 16–43% yields, and identified by ¹H/¹³C NMR and MALDI-TOF-MS. Based on theoretical studies at B3LYP/6-31G(d,p),⁸ the *anti* conformation of the two NH sites in 2,2'-bipyrrrole, as a core moiety of **2a-d** and **3a-d**, was more stable at 2.78 kcal mol⁻¹ than the corresponding *syn* conformation, whereas the *syn* conformation of C=O and pyrrole NH sites in 2-benzoylpyrrole, as a partial moiety of **2a-d** and **3a-d**, was more stable at 4.06 kcal mol⁻¹ than the corresponding *anti* conformation. These results were consistent with the appropriate orientations of dipoles in the building units as well as the preferred conformations of benzoyl-substituted bipyrroles. The bipyrrrole derivatives, mainly existing as more symmetric *anti* conformations, would be suitable building units for the formation of aggregates. In fact, changes in the variable temperature (VT) UV/vis absorption spectra of **3c** in octane (1 mM) showed two-step transitions upon cooling (Fig. 2a). Upon cooling from 80 to 0 °C, the absorption at around 400 nm was red-shifted, suggesting that the molecular conformation was fixed to provide

^a Department of Applied Chemistry, College of Life Sciences, Ritsumeikan University, Kusatsu 525-8577, Japan. E-mail: maedahir@ph.ritsumei.ac.jp

^b Research and Utilization Division, Japan Synchrotron Radiation Research Institute, Sayo 679-5198, Japan

† Electronic supplementary information (ESI) available: Synthetic procedures, DSC profiles, POM images, XRD patterns and CIF files. CCDC 1474906 and 1474907. For ESI and crystallographic data in CIF or other electronic format see DOI: 10.1039/c6cc03423c

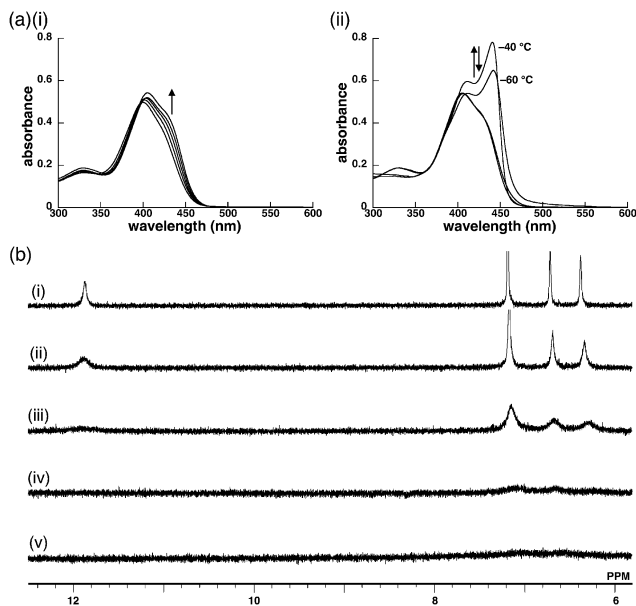


Fig. 2 (a) Changes in variable temperature (VT) UV/vis absorption spectra of **3c** in octane (1 mM) upon cooling from (i) 80 to 0 °C and (ii) 0 to –60 °C and (b) changes in VT ^1H NMR spectra of **3c** in octane- d_{18} (1 mM) upon cooling from (i) 40 to (v) –40 °C via (ii) 20, (iii) 0 and (iv) –20 °C.

planar geometries. Further cooling from 0 to –60 °C caused a new band to appear at 440 nm, ascribed to the formation of aggregates. VT ^1H NMR spectral changes of **3c** in octane- d_{18} (1 mM) showed broad less clear signals at lower temperatures, suggesting the formation of aggregates (Fig. 2b).

Single-crystal X-ray analysis of **2a** and **3a** showed their solid-state molecular conformations and assemblies (Fig. 3), especially using synchrotron radiation X-rays at BL40XU SPring-8 for **3a**.^{‡,§} Molecules in the solid state showed similar conformations, as seen in theoretical studies. The two pyrrole units in bipyrrrole moieties

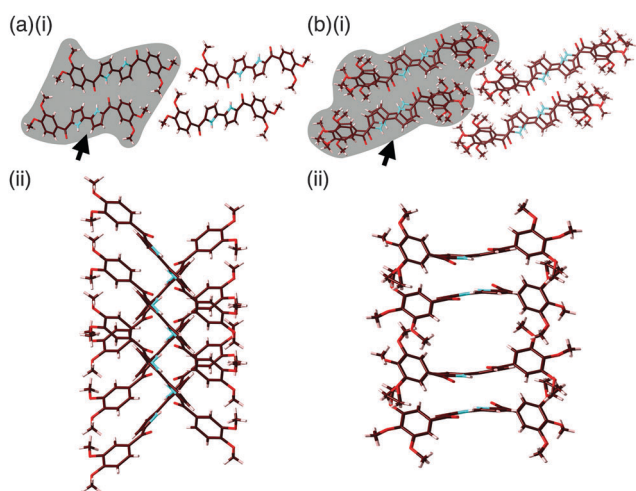


Fig. 3 Single-crystal X-ray analysis of (a) **2a** and (b) **3a** as assembled structures as (i) top views showing intermolecular N–H...O=C hydrogen bonding and (ii) side views of columnar structures from the directions of arrows in (i). Atom colour code: brown, pink, blue and red refer to carbon, hydrogen, nitrogen and oxygen, respectively.

with *anti* orientations had dihedral angles of 0° (completely parallel) and 11.58° for **2a** and **3a**, respectively,¹⁰ whereas benzoyl units, whose C=O moieties were oriented in the same direction as pyrrole NH, resulted in distortions in the core bipyrrrole unit, with dihedral angles of 33.0° and 58.0°/51.4° for **2a** and **3a**, respectively. On the other hand, columnar structures of **2a** and **3a** were constructed by aggregation, with repeat π -plane distances of 3.38 Å and 3.37/7.33 Å, respectively. In the packing structures, **2a** formed tilted columnar structures, whose components have a dihedral angle of 85.9° with those in neighbouring columns (Fig. 3a), whereas, in **3a**, disordered solvents expanded the distance between two molecules (Fig. 3b). Columns of **2a** and **3a** were arranged in 1D chain-like forms through hydrogen bonding with N(H)...O(=C) distances of 2.88 Å and 2.99 Å, respectively. Notably, pyrrole NH units in the columnar structures were oriented in the same direction for both **2a** and **3a** in the stacking pairs.

Bipyrrroles **2b–d** and **3b–d**, possessing aliphatic chains, afforded yellow or yellowish-green solids from $\text{CHCl}_3/\text{MeOH}$. The thermal transition behaviours of **2b–d** and **3b–d**, examined by differential scanning calorimetry (DSC), were dependent on the number and length of aliphatic chains (Table 1). DSC of **2b–d** and **3b–d** showed thermal transitions at temperatures (°C) of 168/4 and 8/173 (**2b**), 153/134/27 and 31/153 (**2c**), 147/40 and 39/107/118/145 (**2d**), 83 and 58/93 (**3b**), 68/56 and 55/65/74 (**3c**), and 60/33/20 and 48/61 (**3d**), upon 1st cooling and 2nd heating, respectively, suggesting the formation of mesophases. Polarized optical microscopy (POM) of **2b** showed fibre-like textures upon cooling from the isotropic liquid (Iso), whereas POM of **2c** and **2d** as mesophases showed coffee bean-like textures (Fig. 4a). On the other hand, **3b–d** mesophases exhibited mosaic-like textures *via* POM.

Synchrotron X-ray diffraction (XRD) analysis (BL40B2, SPring-8) of **2c** showed three mesophases, including two lamellar phases and a rectangular columnar (Col_r) phase at 10, 80 and 140 °C, respectively, upon cooling (Fig. 4b). The two lamellar phases exhibited layer distances of 2.93 and 3.32 nm at 10 and 80 °C, respectively, suggesting that the shorter distance at low temperature was due to effective interactions. At higher temperatures, the changes in molecular orientations and interdigitation between aliphatic chains resulted in another lamellar phase, supported by π - π stacking and van der Waals interactions for core units and aliphatic chains, respectively, with a layer distance that was approximately equal to the tilted orientation (*ca.* 45°) for the molecular length (4.85 nm)⁸ providing $4.85/\sqrt{2} = 3.43$ nm. Furthermore, the minimum layer distance formed by vertically oriented molecules was *ca.* 3.3 nm in a completely interdigitated form, suggesting that the layers should form in a tilted orientation. At 140 °C, a Col_r phase was constructed through van der Waals interaction with parameters $a = 5.95$ nm, $b = 3.93$ nm and $c = 0.38$ nm based on a single molecule in the unit disc ($Z = 4$ for $\rho = 0.8$). The space for one molecule became larger with increasing mobility of the constituent molecules, resulting in low densities at high temperatures. On the other hand, upon cooling, XRD of **2d**, possessing four long alkyl chains, showed three mesophases, comprising two lamellar phases and a Col_r phase at 40,

Table 1 Summary of transition behaviours for **2b–d** and **3b–d**

	Cooling ^a	Heating ^a
2b	Cr ^b 4 Cr ^b 168 Iso	Cr ^b 8 Cr ^b 174 Iso
2c	lamellar 27 lamellar 134 Col _r 153 Iso	lamellar 31 lamellar 154 ^c Iso
2d	lamellar 40 lamellar 110 ^d Col _r 147 Iso	lamellar 39 lamellar 107 lamellar 118 Col _r 145 Iso
3b	Col ^e 84 Iso	Col ^e 58 Col _{tet} 93 Iso
3c	Cr ^f 56 Cr ^f 68 Iso	Cr ^f 55 Cr ^f 74 Iso
3d	Col _{tet} 10 Col _{tet} 33 Col _{hex} 61 Iso	Col _{tet} 48 Col _{hex} 61 Iso

^a Transition temperatures (°C, peak onset) from DSC 1st cooling and 2nd heating scans (5 °C min⁻¹). ^b Cr with lamellar-based unidentified structure. ^c Col_r phase was exhibited before melting as identified using XRD patterns. ^d Transition temperature of the broad peak was supported by the change in XRD patterns. ^e Col_{tet} and Col_{hex} mixed phases, depending on the cooling processes. ^f Cr with unidentified structures.

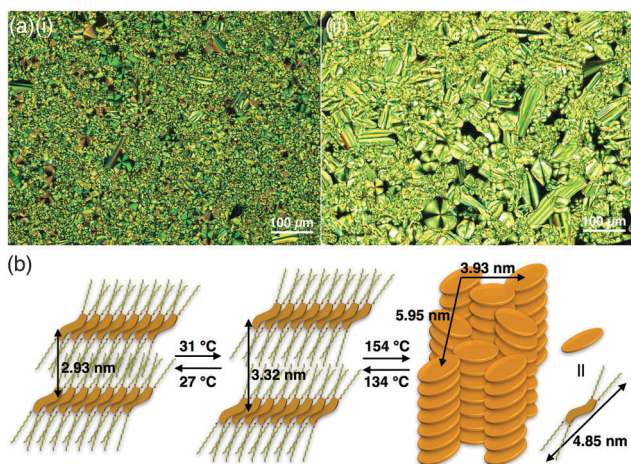


Fig. 4 (a) POM textures of (i) **2c** at 153 °C and (ii) **2d** at 147 °C upon cooling and (b) possible assembled models of **2c**.

110 and 147 °C, respectively. The two lamellar phases were fabricated by the layers with distances of 3.81 and 3.97 nm at 25 and 100 °C, respectively. At 120 °C, a Col_r phase was formed by van der Waals interaction with the parameters $a = 6.50$ nm, $b = 2.98$ nm and $c = 0.39$ nm based on a single molecule in the unit disc ($Z = 2$ for $\rho = 0.6$). The formation of tilted columns of **2c** and **2d** in the Col_r phases correlated with the single-crystal X-ray structure of **2a**. In contrast to **2c** and **2d**, **2b** exhibited complicated XRD patterns because shorter aliphatic chains in **2b** allowed more effective intermolecular interactions.

The number of aliphatic chains in benzoyl-substituted bipyrroles was important for influencing dimension-controlled assemblies. Synchrotron XRD of **3b** suggested the formation of two mesophases at 70 °C upon cooling, namely, hexagonal columnar (Col_{hex}) and tetragonal columnar (Col_{tet}) phases, with the unit parameters $a = 2.82$ and 2.06 nm, respectively, and $c = 0.77$ nm in both cases. The Col_{hex} and Col_{tet} phases were fabricated from trimeric ($Z = 3$ for $\rho = 1$) and dimeric ($Z = 2$ for $\rho = 1.2$) unit discs, respectively (Fig. 5a). Upon cooling from the Iso, a phase containing both Col_{tet} and Col_{hex} structures was observed. Through time-dependent changes in the XRD patterns,

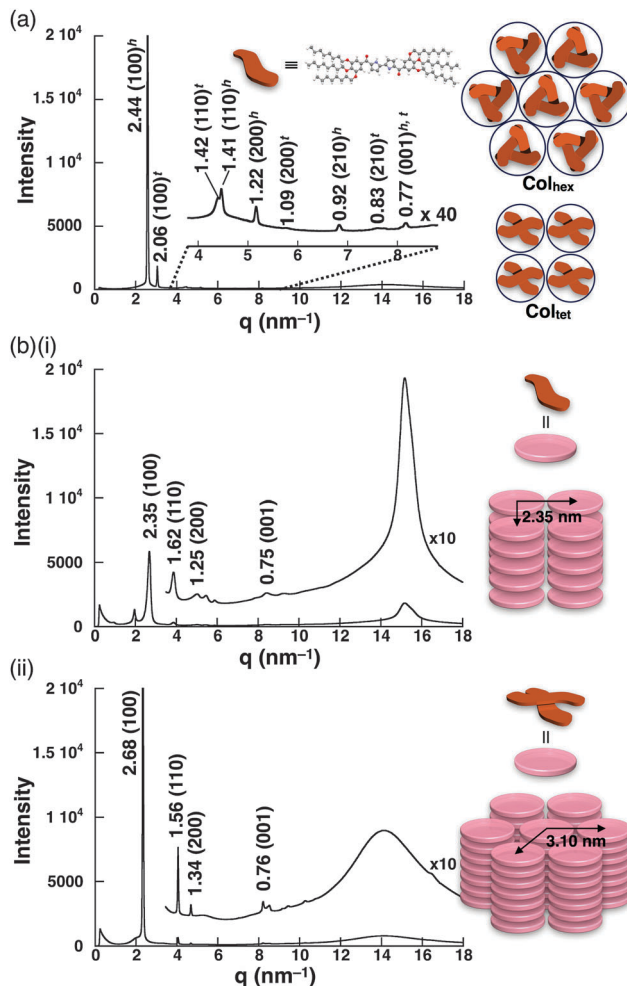


Fig. 5 (a) XRD pattern of **3b** at 70 °C upon cooling and possible assembled models, wherein Col_{hex} and Col_{tet} phases consisted of trimeric and dimeric unit discs, respectively, and the peaks labeled as *h* and *t* were derived from the respective phases. (b) XRD patterns of **3d** at (i) 28 °C upon cooling and (ii) 45 °C upon cooling and possible assembled models. The sharper halo pattern in the Col_{tet} phase suggested that monomeric disc units induced strong interactions among aliphatic chains.

at 80 °C upon cooling, the peak pattern of the Col_{tet} phase was initially less intense than that of the Col_{hex} phase, but the peak intensity became greater than that of the Col_{hex} phase after annealing at 5 min. Therefore, the Col_{tet} and Col_{hex} phases were found to be in more stable and metastable states, respectively, at this temperature. In contrast, at 40 °C upon cooling, the peak ratio of Col_{hex} to Col_{tet} did not change by annealing. Furthermore, due to rate-dependent changes in the XRD patterns, at 40 °C upon cooling, the peak pattern of the Col_{hex} phase with a cooling rate of 10 °C min⁻¹ was initially more intense than that with a cooling rate of 5 °C min⁻¹. This observation suggested that **3b** might form soft crystals at low temperatures. The balance between the Col_{hex} and Col_{tet} phases can be ascribed to building unit stabilities of the columnar structures; the trimeric assembly in Col_{hex} is kinetically more stable than the dimeric assembly in Col_{tet} upon cooling from the Iso. However, the trimeric assembly in Col_{hex} was thermodynamically less stable than the dimeric

assembly in Col_{tet}, resulting in a phase transition from Col_{hex} to Col_{tet}. Furthermore, the Col_{tet} phase formed above 58 °C upon heating from mixed states, also suggesting that Col_{tet} was more stable than Col_{hex}.

XRD of **3d** exhibited the formation of Col_{tet} and Col_{hex} mesophases at 28 and 45 °C, respectively, upon cooling. The Col_{tet} and Col_{hex} phases, with $a = 2.35$ and 3.10 nm and $c = 0.75$ and 0.76 nm, respectively, consisted of monomeric ($Z = 1$ for $\rho = 0.8$) and dimeric ($Z = 2$ for $\rho = 1$) unit discs, respectively (Fig. 5b). The c values, which were twice the general π - π stacking, revealed the stacking of two molecules with opposite orientations to prevent the overlap of aliphatic chains in stacking molecules in the unit disc of Col_{hex}. The unit disc consisting of a single molecule in Col_{tet} induced effective interactions in the aliphatic chains rather than in the core units, providing a small calculated density of <1 . In contrast to **3b** and **3d**, **3c** exhibited complicated XRD patterns due to its more effective intermolecular interactions than those in **3b** and **3d**. The larger number of flexible points (alkoxy oxygens) in **3b-d** may require longer aliphatic chains for effective intermolecular interactions, those for π -units, polarized NH and CO units and aliphatic chains, compared to **2b-d**.

In summary, benzoyl-substituted bipyrrrole derivatives were found to form dimension-controlled assemblies through intermolecular interactions. Tetraalkoxy-substituted **2c** and **2d** formed lamellar and tilted Col_r structures, whereas hexaalkoxy-substituted **3b** and **3d** formed mainly vertically oriented Col_{tet} and Col_{hex} structures. Multiple interactions were present in the pyrrole-based molecules, enabling a variety of assembly modes depending on the numbers and lengths of aliphatic chains. Interactions between dipoles of constituent π units, which are not easy to examine in order to discuss in detail, are essential for the formation of assemblies. Further modifications and molecular design will provide fascinating dimension-controlled assembled structures.

This work was supported by Grants-in-Aid for Scientific Research (B) (No. 26288042) and on Innovation Areas ("Photo-synergetics" Area 2606, No. 26107007) from the MEXT. We thank Prof. Atsuhiko Osuka and Mr Takanori Soya, Kyoto University, for single-crystal X-ray analysis, Prof. Hikaru Takaya, Kyoto University, and Dr Ryohei Yamakado, Ritsumeikan University, for synchrotron radiation XRD measurements (BL40XU at SPring-8: 2015A1388), Dr Noboru Ohta, JASRI/SPring-8, for synchrotron radiation XRD measurements (BL40B2 at SPring-8),

Prof. Tomonori Hanasaki, Ritsumeikan University, for POM measurements and Prof. Hitoshi Tamiaki, Ritsumeikan University, for various measurements.

Notes and references

‡ Crystal data for **2a** (from EtOAc/*n*-heptane): C₂₆H₂₄N₂O₆, $M_w = 460.47$, monoclinic, $P2_1/c$ (no. 14), $a = 15.361(4)$ Å, $b = 4.9550(13)$ Å, $c = 14.843(4)$ Å, $\beta = 98.245(7)^\circ$, $V = 1118.1(5)$ Å³, $T = 93(2)$ K, $Z = 2$, $D_C = 1.368$ g cm⁻³, $\mu(\text{Cu-K}\alpha) = 0.809$ mm⁻¹, $R_1 = 0.0329$, $wR_2 = 0.0938$, GOF = 1.074 ($I > 2\sigma(I)$). CCDC 1474906. Crystal data for **3a** (from EtOAc/*i*Pr₂O): C₂₈H₂₈N₂O₈·C₄H₈O₂, $M_w = 520.54$, triclinic, $P\bar{1}$ (no. 2), $a = 7.9706(19)$ Å, $b = 10.519(3)$ Å, $c = 17.440(4)$ Å, $\alpha = 87.803(4)^\circ$, $\beta = 86.847(4)^\circ$, $\gamma = 78.375(4)^\circ$, $V = 1429.4(6)$ Å³, $T = 90(2)$ K, $Z = 4$, $D_C = 1.312$ g cm⁻³, $\mu(\text{synchrotron radiation}) = 0.120$ mm⁻¹, $R_1 = 0.0551$, $wR_2 = 0.1213$, GOF = 1.132 ($I > 2\sigma(I)$). CCDC 1474907.

- (a) *Supramolecular Polymers*, ed. A. Ciferri, Marcel Dekker, New York, Basel, 2000; (b) G. A. Ozin and A. C. Arsenault, *Nanochemistry: A Chemical Approach to Nanomaterials*, RSC, Cambridge, 2005; (c) *Supramolecular Dye Chemistry, Topics in Current Chemistry*, ed. F. Würthner, Springer, Berlin, 2005, vol. 258, pp. 1–324.
- (a) M.-C. Yeh, Y.-L. Su, M.-C. Tzeng, C. W. Ong, T. Kajitani, H. Enozawa, M. Takata, Y. Koizumi, A. Saeki, S. Seki and T. Fukushima, *Angew. Chem., Int. Ed.*, 2013, **52**, 1031–1034; (b) A. El-Ghayoury, L. Zorina, S. Simonov, L. Sanguinet and P. Batail, *Eur. J. Org. Chem.*, 2013, 921–928; (c) J. Wudarczyk, G. Papamokos, V. Margaritis, D. Schollmeyer, F. Hinkel, M. Baumgarten, G. Floudas and K. Müllen, *Angew. Chem., Int. Ed.*, 2016, **55**, 3220–3223.
- (a) E. J. Foster, C. Lavigueur, Y.-C. Ke and V. E. Williams, *J. Mater. Chem.*, 2005, 4062–4068; (b) H. Maeda, Y. Kusunose, M. Terasaki, Y. Ito, C. Fujimoto, R. Fujii and T. Nakanishi, *Chem. – Asian J.*, 2007, **2**, 350–357; (c) R. J. M. Courtemanche, T. Pinter and F. Hof, *Chem. Commun.*, 2011, **47**, 12688–12690; (d) S. Ward, O. Calderon, P. Zhang, M. Sobchuk, S. N. Keller, V. E. Williams and C.-C. Ling, *J. Mater. Chem. C*, 2014, **2**, 4928–4936.
- (a) D. T. Gryko, *Eur. J. Org. Chem.*, 2002, 1735–1743; (b) S. Fukuzumi, K. Ohkubo, M. Ishida, C. Preihs, B. Chen, W. T. Borden, D. Kim and J. L. Sessler, *J. Am. Chem. Soc.*, 2015, **137**, 9780–9783.
- T. Dohi, M. Ito, N. Yamaoka, K. Morimoto, H. Fujioka and Y. Kita, *Tetrahedron*, 2009, **65**, 10797–10815.
- K. C. Braaten, D. G. Gordon, M. M. Aphibal and G. R. Geier, III, *Tetrahedron*, 2008, **64**, 9828–9836.
- (a) N. Schröder, J. Wencel-Delord and F. Glorius, *J. Am. Chem. Soc.*, 2012, **134**, 8298–8301; (b) A. S. Kumar, B. Thulasiram, S. B. Laxmi, V. S. Rawat and B. Sreedhar, *Tetrahedron*, 2014, **70**, 6059–6067.
- M. J. Frisch, *et al.*, *Gaussian 09 (Revision D.01)*, Gaussian, Inc., Wallingford CT, 2009.
- (a) N. Yasuda, H. Murayama, Y. Fukuyama, J. E. Kim, S. Kimura, K. Toriumi, Y. Tanaka, Y. Moritomo, Y. Kuroiwa, K. Kato, H. Tanaka and M. Takata, *J. Synchrotron Radiat.*, 2009, **16**, 352–357; (b) N. Yasuda, Y. Fukuyama, K. Toriumi, S. Kimura and M. Takata, *AIP Conf. Proc.*, 2010, **1234**, 147–150.
- The conformations in the solid state were quite different from the *syn* conformation in perfluorobenzoyl-substituted bipyrrrole derivatives: T. Hong, H. Song, X. Li, W. Zhang and Y. Xie, *RSC Adv.*, 2014, **4**, 6133–6140.